Indian Journal of Pure & Applied Physics
Vol. 63, September 2025, pp. 788-795
DOI: 10.56042/ijpap.v63i9.14279

A review

Cathode Material for Solid Oxide Fuel Cell: A review

Surinder Paul[a *], Sangeeta Devi[b], Aman Sen[a], Shruti Rialach[a] & Manokamna[c]

[a]Department of Physics & Astronomical Science, Central University of Himanchal Pradesh, Dharamshala1 761215, India

[b]Department of Physics, Arni University, Indora 176 402, India

[c]Department of Education, Government of Himachal Pradesh, Shimla 171 001, India

Received:9th Oct 2024; accepted:9th July 2024

Solid oxide fuel cell (SOFC) technology heralds a paradigm shift in energy conversion by seamlessly transforming chemical energy into electrical power without resorting to combustion. The core constituent's anode, electrolyte, and cathode-work synergistically within the stack, culminating in a substantial power output. Positioned between the anode and cathode, the electrolyte facilitates the movement of O^{2-} ions sans the requirement for external electron circuits. At the anode, oxidation transpires, while reduction transpires at the cathode. Operating within a temperature spectrum of 450 to 1000°C, SOFCs not only furnish high-grade heat but also expedite electro catalysis through commonplace metals, thereby fostering internal reorganization. SOFCs, boasting remarkable efficiency, thrive on materials evincing high electrical conductivity, ensuring smooth electron transfer and amplifying overall cell performance. The technology's promise for clean and efficient energy conversion is undeniable. By leveraging suitable materials and operating within specified temperature ranges, SOFCs emerge as a potent force in diverse energy sectors. Continuous research endeavors aim to refine and optimize SOFC components, bolstering their efficacy and practical applicability. The analysis delves into various material attributes such as mechanical robustness, thermal expansion coefficients, electrochemical behavior and electrical conductivity. The composition's dopants and their valence significantly influence cathode characteristics, categorizing materials into cobalt-based or cobalt free variants. While cobalt-based iterations typically exhibit superior conductivity, cobalt-free alternatives offer cost-effectiveness and comparable thermal expansion coefficients. The discourse concludes by outlining avenues for future research, underscoring the perpetual quest to enhance SOFC performance and realize their vast potential in revolutionizing energy conversion technologies.

Keywords: SOFC, Cathode materials, Conductivity, Fuel cell, Electrochemical process

1 Introduction

Using electrochemical processes, fuel cells are novel technologies that provide a clean and effective substitute for conventional combustion-based power generating techniques. They transform chemical energy directly into electrical energy. With roots tracing back to the 19th century, fuel cell technology has evolved significantly, driven by advancements in materials science and engineering. These devices operate by combining hydrogen or other fuels with oxygen from the air, producing electricity, heat, and water as by products. With diverse applications ranging from transportation to stationary power generation, fuel cells represent a promising solution to the problems of climate change and sustainability of energy in the twenty-first century, in the contemporary era, SOFC technology is gaining remarkable traction due to its exceptional power production capabilities and high electrical performance, catering to residence and automotive needs[1,2,3]. As an electrochemical device, fuel cells promise significant environmental benefits and efficient electric power generation[4,5]. SOFCs stand out among fuel cell variants, offering advantages such as fuel adaptability, impressive energy conversion efficiency unaffected by the Carnot Cycle limitations, minimal chemical pollution, reduced gas emissions, and simultaneous heat and electricity generation. Positioned as an ideal choice for clean power generation, SOFCs emerge as pivotal in the transition toward sustainable energy solutions, underlining their significance in modern energy landscapes. Because SOFCs do not require lubrication, leakage, or heat loss, they surpass conventional heat engines[6,7]. An individual fuel cell is made up of a cathode and an anode that are divided by an electrolyte made up of solid oxide, as seen in Fig. 1[8,9].

The anode is continually supplied with fuel, such H_2 or CH_4, while the cathode is fed by an oxidant. At the anode, fuel undergoes decomposition into positive and negative ions. As an insulator, the electrolyte only permits protons, or cations, to move from the anode to

*Corresponding author: E-mail: surinderpaul79@hpcu.ac.in

cathode. External circuits help free electrons recombine on the cathode side, which stabilizes the system. The electrons produce during the oxidation of fuel at the anode is utilized for reduction of oxygen at the cathode, thus finalizing the external circuit and producing electricity. In practical applications, numerous fuel cells are grouped together to enhance power output, with the intermediate electrolyte bridging the space among the anode and cathode, facilitating ion transfer[11-13]. This arrangement maximizes power generation efficiency and pivotal role in SOFCs, facilitating the entry of air (oxygen) into the cell where it undergoes conversion into ions (O^{2-}). This transformation, termed as oxygen reduction reaction (ORR), occurs at a specific region called the triple-phase boundary (TPB), as depicted in Fig. 2[14]. At the TPB, oxygen gas is reduced to O^{2-} ions, which then traverse toward the electrolyte from cathode and subsequently into the electrolyte lattice. The length of the TPB significantly influences SOFC performance, with a longer TPB enhancing reaction rates and overall cell efficiency. However, if any phase within the TPB breaks down, the reaction cannot proceed[15,16], thereby affecting cell performance and contributing to total cell resistance. The arrangement and composition of SOFC components impact the size and apportionment of TPBs, impacting cell operation.

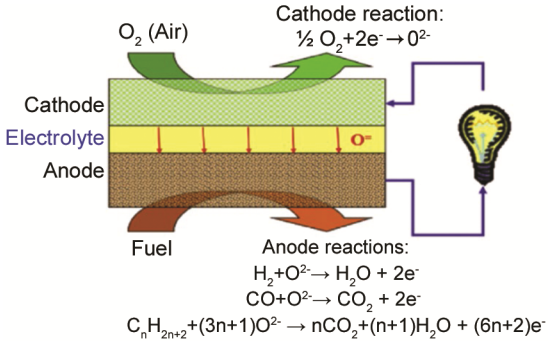

Fig. 1 — Schematic representation of solid oxide fuel cellLLC[10]

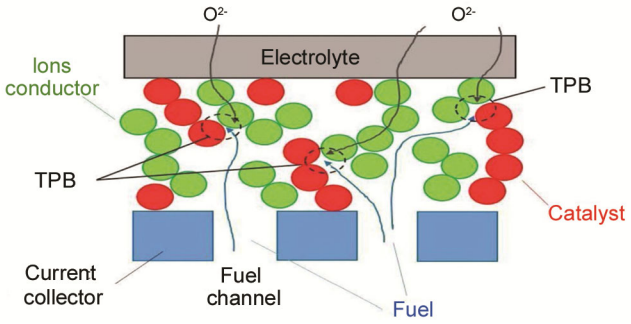

Fig. 2 — Schematic diagram of triple-phase boundary at cathode[29]

Oxygen reduction and ion incorporation into the electrolyte may occur through surface or bulk pathways, as discussed extensively by Adler[18-20]. Understanding the mechanisms governing the ORR is crucial for optimizing SOFC design and enhancing overall performance. Extensive research endeavors focus on developing cost-effective cathode materials to advance SOFC commercialization, recognizing their pivotal role in SOFC performance. This article offers an overview of perovskite-based materials deemed promise cathode candidates for SOFCs.

2 Cathode Requirements

In SOFCs, the cathode operates as the location for the electrochemical reduction of oxygen. For this consequence, the cathode must possess: (i) elevated electronic conductivity in an oxidizing environment, preferably more than 100 S cm^{-1}; (ii) thermal expansion coefficient (TEC) that is harmonious with the electrolyte and connection components, as well as their chemical compatibility; (iii) sufficient permeability to enable easily permeate of oxygen gas through the cathode and reach the contact between the cathode and electrolyte; (iv) stability throughout manufacturing and operation in an oxidizing environment; (v) strong oxygen reduction reaction (ORR) catalytic activity; and (vi) inexpensive . The preferred cathode material for heightened temperature SOFCs, which generally function between 800 and 1000°C, is a combination of yttria-stabilized zirconia (YSZ) and Sr-substituted LaMnO3 (LSM). There have also been other mixed ionic-electronic conductors (MIECs) utilized as the cathode; these are covered later. The temperature at which the electrolyte has enough ionic conductivity to function is what determines the working temperature of SOFCs. Additionally, the electrolyte materials used which must be carefully chosen to meet TEC and prevent unwanted intersection reactions-have a notable impact on the choice of cathode materials. Zirconia stabilized with yttria is the electrolyte material most frequently employed due to their elevated ionic conductivities at lower working temperatures. Other oxides such lanthanum strontium gallium magnesium oxide (LSGM), gadolinia-doped ceria (GDC), and Scandia stabilized zirconia samaria-doped ceria (SDC) are also being considered.

3 Perovskite Structure Cathode Systems

With A and B-cations integrated within its structure, the ABO_3 perovskite structure has special

qualities. A-cations, which usually consist of cations from group 13-15, elements from the 6th row, rare-earth, alkaline earth metals, and alkali, occupy the bigger spaces and form a close-packed cubic structure with O^{2-} ions. B-cations, on the other hand, fill octahedral spaces and affect the material's electrical characteristics. Broad energy bands are formed inside the perovskite as a consequence of the interaction among the transition metals d-orbitals and oxygen's 2p-orbitals. Distortions in the perovskite structure, often induced by doping with rare earth ions, affect its electronic properties and conductivity. For instance, increasing distortion through rare earth metal doping can enhance conductivity, with larger cations like La, Ce, and Pr demonstrating higher conductivity due to their larger ionic radii[21,22]. The choice of cathodic material in perovskite structures depends on the transition metal oxide's oxidation state. Transition metals with higher oxidation states (4d and 5d) exhibit higher conductivity, such as niobium, compared to 3d elements like $LaTiO_3$, which are unstable in oxidizing environments. To enhance conductivity, heterovalent substitution of La^{3+} with Sr^{2+}, Ca^{2+}, or Ba^{2+} can increase charge carrier concentration. SOFC cathode materials' TEC has a significant impact on how well they work with the other components. Temperature rises result in increased oxygen vacancies and improved metal-oxygen bonding, which in turn drive thermoelectric and magnetic characteristics that determine thermoelectric conductivity (TEC). Materials like $LaCoO_3$ demonstrate high TEC due to spin transitions between high and low-spin states of Co^{3+} cations. However, Co-perovskites are reactive with YSZ-based electrolytes, requiring protective layers like GDC to mitigate reactivity. While GDC layers provide protection, they introduce diffusion complexities during long-term SOFC operation[23]. Alternately, reactivity can be decreased by partially substituting Mn, Ni, Fe, or Cu for Co in place of other B-site cations. As an example, $La_{1-x}Sr_xCoO_{3-\delta}$ composites show high TEC (15.4 ppm/K) and conductivity (> 100 S/cm) at 800°C, as well as oxygen diffusion rate and catalytic performance that support effective fuel cell operation[24-26]. ABO_3 perovskite structures offer versatile electronic and conductivity properties, influenced by A and B-cation compositions and structural distortions. By taking into account these characteristics, cathode materials for SOFCs may be designed with maximum performance in mind,balancing conductivity, reactivity, and compatibility with other components.

4 La-based Materials

Perovskite substances, specifically those of the $LaMO_3$ variety where M represents a d-block metal, exhibit a blend of ionic and electronic conductivity. Research by Kim *et al*.[27] highlights how oxides like $LnBaCo_2O_{5+\delta}$ (where Ln = Nd, La, Gd, Sm, and Y) demonstrate a fall in oxygen level, TEC, and electrical conductivity as the dimension of Ln^{3+} ions decrease from La to Y in the system. This decline in TEC stems from diminishing ionicity in Ln-O bonds at the expense of covalent bonding, whereas decline in electrical conductivity is attributed to the curving of O-Co-O bonds, altering the bond angle among cobalt and oxygen within octahedral coordination. Notably, TEC and conductivity values remain high within the span of 80-900°C. Specifically, the minimum TEC value, occurring between 500-900°C, measures $14.9\times10^{-6}K^{-1}$ for Ln = Y, indicative of lesser oxygen reduction from the lattice. Contrastingly, the cubic double perovskite oxide $LaSrMnCoO_{5+\delta}$, as explored by Zhou and colleagues[28], display a mean TEC of $15.8\times10^{-6}K^{-1}$ within the 30-1000°C range, albeit higher than conventional electrolyte materials like YSZ, SDC and LSGM. Despite this, its electrical conductivity falls between 111-140 S cm^{-1} at 600-850°C,lower than cobaltite cathodes like $LnBaCo_2O_{5+\delta}$.The thermal expansion data confirm structural stability with SDC within the 600-850◦C range. Vacancies typically enhance overall conductivity, yet oxygen vacancy ordering can paradoxically decrease system conductivity, as examined by Shen and colleagues[29]. Their investigation into cathode composition $La_{0.6}Sr_{0.4}Co_{0.2}Fe_{0.8}O_3$, $Ba_{0.5}Sr_{0.5}Co_{0.2}Fe_{0.8}O_3$, and $Sm_{0.5}Sr_{0.5}Co_{0.2}Fe_{0.8}O3$-revealed maximal conductivity (176 S cm^{-1} at 300°C) for $La_{0.6}Sr_{0.4}Co_{0.2}Fe_{0.8}O_3$,with other samples exhibiting conductivity between 4-50 S cm^{-1}. Similarly, Wu *et.al*.[30] explored physical properties of lanthanum-based $La_{1-x}Sr_xCoO_{3-\delta}$,noting conductivity varying from typical semiconductor to metallic behavior, reaching 1867 S cm^{-1} at 800°C for x = 0.4, consistent with literature. Lanthanum-based $La_{1-x}Sr_xCoO_{3-\delta}$ specimen with x = 0.3 and x = 0.4 exhibit TECs near to between $18-20\times10^{-6}K^{-1}$ within 300-750°C, suitable for low-temperature SOFCs. However, significant differences in TEC compared to standard electrolyte materials may induce mechanical stresses and micro-cracks in SOFC interfaces.

Conductivity measurements of LaBaCo2O5+δ reveal a temperature dependent behavior, peaking at 250°C, but declining thereafter due to lattice oxygen release and Co^{4+} ion reduction. Li *et.al.*[31] investigated $La_{0.5}Ba_{0.5}Co_{1-y}Fe_yO_{3-\delta}$, noting conductivity reduce with elevating Fe quantity, while TEC trends downward for specimen with x = 0.3, 0.5, and 0.7. Aspecimen with y = 0.1 exhibits superior electrochemical effectiveness at 650-750°C, with peak conductance (800 S cm^{-1} at 227°C) double that noted elsewhere. Gedziorowski *et al*. [32] studied Ba-doped $La_{1-x}Ba_xCo_{0.2}Fe_{0.8}O_{3-\delta}$, finding increased oxygen non-stoichiometry with higher Ba content, which reduces perovskite structure distortion. However, even the specimen with x =0.4, despite its elevated conductivity, falls short of the required level for SOFC applications. Notably, systems with Ba dopants exhibit lower conductivity than Sr-doped counterparts.

5 Pr-based Materials

The synthesis and examination of various double perovskite Pr-based materials for potential use in SOFCs have been extensively explored in recent research. One such material, $Pr_{0.4}Sr_{0.6}(Co_{0.2}Fe_{0.8})_{1-x}Mo_xO_{3-\delta}$ (PSCF), synthesized via solid-state reaction, exhibited varying TEC in the midst of 13.44 to 15.06 × $10^{-6}K^{-1}$ in the temperature scale of 100-500°C. The highest TEC was noted for x=0.05 composition, correlating with the peak conductivity of 128.8 S cm^{-1} at 850°C. There is decrease in conductivity with increasing Mo quantity due to the suppression of Fe^{4+} and Co^{3+} states by B-site cations, leading to fewer charge carriers. Similarly, $(Pr_{0.6}Sr_{0.4})_{1-x}Fe_{0.8}Co_{0.2}O_{3-\delta}$ compositions without Mo doping exhibited conductivity values of 402 S cm^{-1} at 520°C, with a linear decrease in TEC attributed to cobalt loss from the perovskite structure. Meng*et.al.*, studied $Pr_{1-x}Sr_xCo_{0.8}Fe_{0.2}O_{3-\delta}$ with varying Sr content, reporting conductivity exceeding 279 S cm^{-1}, reaching 1040 S cm^{-1} at 300°C for x=0.4. However, high TEC values between 30-850°C (up to$21.23\times10^{-6}K^{-1}$) posed challenges, prompting the fabrication of composite cathodes to match TEC with electrolyte materials. Jiang et al. observed decreased TEC values (21.3 to $19.2\times10^{-6}K^{-1}$) for $PrBaCo_{2-x}Fe_xO_{5+\delta}$ $6.6\times10^{-6}K^{-1}$) and increased conductivity (144 S cm^{-1} at 600°C), attributed to Co substitution by Fe and Cu, inducing spin flip of Co^{3+} ions and more potent Fe-O bonds. Zhao *et al*. studied iron-doped $PrBaCo_{2-x}Fe_xO_{5+\delta}$, noting increased lattice parameters and decreased TEC with Fe doping, emphasis compositions, attributing increased conductivity (60-769 S cm^{-1}) to smaller lattice volumes from Sr^{2+} substitution. Fe/Co molar ratio variation revealed significant TEC reduction ($21.3\times10^{-6}K^{-1}$ to $19.2\times10^{-6}K^{-1}$) due to lattice expansion with Fe substitution. Jin*et.al*. reported $PrBaCo_{2/3}Fe_{2/3}Cu_{2/3}O_{5+\delta}$ with lower TEC (1ing higher energy requirements for Fe reduction. Park *et.al*. investigated Sr-doped $PrBa_{1-x}Sr_xCo_2O_{5+\delta}$, synthesized via the Pechini process, reporting the highest electrical conductivity among Pr-based double perovskites (300-3000 S cm^{-1}) due to increased oxygen content from Sr doping and crystal structure ordering. Moderate TEC values were observed, making these materials suitable for SOFC applications.

6 Nd-based Materials

Researchers have extensively investigated compounds containing Nd with the basic composition $NdBaCoO_{5+\delta}$, exploring various dopants and substitutions to understand their structural and functional properties. Dasgupta*et.al.*[33] examined $Nd_{0.7}Sr_{0.3}Fe_{1-x}Co_xO_3$ (x=0-0.8), revealing an orthorhombic crystal structure akin to $GdFeO_3$.Substituting Fe with Co expanded the lattice, increasing thermal expansion, observed through heightened slope in thermal expansion curves. The TEC ranged from 573 to 973°C, with conductivity peaking at 775°C for x=0.4, attributed to Co^{3+} charge disproportionation generating additional charge carriers with rising temperature. Kim *et.al.*[34] investigated Sr doping effects on Nd-based compounds, studying $NdBa_{1-x}Sr_xCoO_{5+\delta}$ (x=0, 0.5). Composite studies with $Ce_{0.9}Gd_{0.1}O_{2-\delta}$ revealed TEC values of 13.2 × 10−6K^{-1} and $12.4\times10^{-6}K^{-1}$ at 600°C for 50 wt.% $NdBa_{0.5}Sr_{0.5}CoO_{5+\delta}$ and$NdBa_{0.5}CoO_{5+\delta}$, respectively. Without $Ce_{0.9}Gd_{0.1}O_{2-\delta}$, TEC exceeded 22 × $10^{-6}K^{-1}$ at 530°C due to network formations. Sr-doped $NdBa_{0.5}Sr_{0.5}CoO_{5+\delta}$ exhibited higher cathodic polarization, attributed to oxygen disorder due to Sr addition. Kim and colleagues[35] explored Mn doping effects on electrochemical characteristics of $NdBa_{0.5}Sr_{0.5}Co_{2-x}Mn_xO_{5+\delta}$ (x=0, 0.25, 0.5), noting high conductivity (200-3000 S cm^{-1}). Mn absent samples displayed metallic conductivity, while doped specimen exhibited semiconducting behavior due to lattice oxygen loss. Mn substitution reduced electrical conductivity but improved thermal expansion due to more potent Mn-O bonding. Yi and colleagues[36] investigated A-site deficiency effects on $Nd_{1-x}Ba_xCo_2O_{6-\delta}$ (x=0, 0.04), revealing comparable TEC values ($20\times10^{-6}K^{-1}$ for x=0, $21.6\times10^{-6}K^{-1}$ for x=0.04) inthe span of 50 to 800°C. High TEC resulted from oxygen vacancy formation and

lattice oxygen loss. Conductivity exceeded 370 S cm^{-1}, slightly reduced by A-site deficiency due to increased oxygen vacancies. This conductivity was lowerthan Ba-deficient $NdBa_{1-x}Co_2O_{5+\delta}$ (750 S cm^{-1} at 700°C)[37]. Nd-based compounds with various dopants and substitutions exhibit diverse structural and functional properties. Sr and Mn doping influence thermal expansion and electrochemical performance, with Sr doping enhancing cathodic polarization and Mn doping improving thermal expansion at the expense of electrical conductivity. A-site deficiency increases TEC due to oxygen vacancy formation but slightly reduces conductivity. These findings contribute to the understanding of tailored properties for potential applications in various technological fields. The following Table 1 represent the different cathode material prepared up to date.

7 Gd-based Materials

Jo *etal.*[45] reported the lowest coefficient of thermal expansion (TEC) in $GdBaCoCuO_{5+\delta}$ compound, investigating $GdBaCo_{0.66}Fe_{0.66}Cu_{0.66}O_{5+\delta}$ cathode with $Ce_{1.9}Gd_{0.1}O_{1.95}$ electrolyte. Synthesized through the citrate combustion technique, the composition displayed a TEC of $14.6\times10^{-6}K^{-1}$, within the SOFC range. Doping with Fe, Ni, and Cu reduced TEC compared to undoped counterparts by mitigating Co^{3+} spin-state transitions and oxide ion vacancy formation. Li *et.al.*[46] calculated $GdBaCo_2O_{5+\delta}$ conductivity as 512-290 S cm−1 in the midst of 500-800°C, whereas Zhou *et.al.*[47] reported 9-13 S cm^{-1} at 650-800°C for $GdBaCuCo_{0.5}Fe_{0.5}O_{5+\delta}$. These values diminished compared to conventional cathode materials and unadulterated cobalt-based cathodes under analogous circumstances. Kuroda *et al.*[48] studied $GdBa_{0.5}Sr_{0.5}Co_{2-x}Fe_xO_{5+\delta}$, revealing conductivity surpassing 1000 S cm^{-1} above 400°C, with a TEC of $24.01\times10^{-6}K^{-1}$, similar to specific Co-rich, Ba or Sr-incorporating composition. Phillipps and colleagues[49] explored $Gd_{1-x}A_xCo_{1-y}Mn_yO_3$ (A=Sr, Ca) as potential cathodes, observing maximum conductivity of 250 S cm^{-1} for Sr-substituted samples with y=0.1. Most samples exhibited semiconducting behavior, with low-Co variants displaying metallic behavior. High Mn concentration samples showed promising TEC for SOFC electrolyte applications. Gd-based cathode materials demonstrate relatively low TEC in comparison Nd and other cobalt containing samples. However, their conductivity remains lower than previously discussed systems. These findings contribute to understanding material properties for optimizing SOFC components, emphasizing the importance of balancing conductivity and thermal expansion for efficient operation.

Table 1 — Perovskite based cathode material thermal showing electronic conductivity values

Anode Composition	Temperature (°C)	Conductivity (Scm^{-1})	Ref.
$Pr_{0.4}Sr_{0.6}(Co_{0.2}Fe_{0.8})_{1-x}Mo_xO_{3-\delta}$	850	128.8	
$La_{1-x}Ca_xFe_{0.75}Co_{0.25}O_3$	900	100	[38]
$(Pr_{0.6}Sr_{0.4})_{1-x}Fe_{0.8}Co_{0.2}O_{3-\delta}$	520	402	
$LaCoO_{3-\delta}$	900	1259	[39]
$Pr_{1-x}Sr_xCo_{0.8}Fe_{0.2}O_{3-\delta}$	300	1040	
$La_{0.8}Sr_{0.2}CoO_{3-\delta}$	800	1221	[40]
$PrBaCo_{2-x}Fe_xO_{5+\delta}$		769	
$La_{0.8}Sr_{0.2}FeO_{3-\delta}$	600	90	[40]
PrBaCo2/3Fe2/3Cu2/3O5+δ	600	144	
$La_{0.9}Ba_{0.10}Co_{0.50}Fe_{0.50}O_3$	200	136.32	[41]
$PrBa_{1-x}Sr_xCo_2O_{5+\delta}$		3000	
$La_{0.6}Sr_{0.4}Co_{0.8}Fe_{0.2}O_{3-\delta}$	600	489	[42]
$NdBa_{0.5}Sr_{0.5}Co_{2-x}MnxO_{5+\delta}$		3000	
$La_{0.6}Ba_{0.40}Mn_{0.50}Fe_{0.50}O_3$	800	349.25	[43]
$Nd_{1-x}Ba_xCo_2O_{6-\delta}$	800	370	
$La_{0.6}Sr_{0.4}Co_{0.8}Fe_{0.2}O_{3-\delta}$	600	489	[42]
$NdBa_{1-x}Co_2O_{5+\delta}$	700	750	
$La_{0.6}Sr_{0.4}Co_{0.8}Fe_{0.2}O_{3-\delta}$	600	489	[42]
$GdBaCo_2O_{5+\delta}$	500	512	
$La_{0.7}Sr_{0.3}Fe_{0.4}Mn_{0.6}O_3$		116.31	[44]
$GdBaCuCo_{0.5}Fe_{0.5}O_{5+\delta}$	800	13	

8 Rare-earth-based Materials

Sr-doped $LaMnO_3$ (LSM) has garnered extensive attention as a cathode material due to its importance in SOFC development. Westinghouse Co has utilized LSM in their tubular SOFC design[50]. LSM, often exhibiting oxygen-rich or oxygen-lacking nonstoichiometric, is doped with strontium to increase electron-hole proportion and electronic conductivity. However, beyond 30 mol% Sr addition, there is a possibility to produce $La_2Zr_2O_7$ (pyrochlore phase) at the LSM and yttria-stabilized zirconia (YSZ) electrolyte interface[51,52,53]. To prevent pyrochlore phase formation, A-site doping is preferred. Research byIshihara *et.al.*[54] assessed cathodic polarization of $Ln_{0.6}Sr_{0.4}MnO_3$ (Ln= Pr, Nd, La, Gd, Sm, Yb, or Y). Sr-incorporated $PrMnO_3$ demonstrated suitable TEC with YSZ based electrolyte, with $Pr_{0.6}Sr_{0.4}MnO_3$ exhibiting a TEC of $12.0\times10^{-6}K^{-1}$, lower than $La_{0.6}Sr_{0.4}MnO_3$. Moreover, Sr-doped $PrMnO_3$, $NdMnO_3$, and $SmMnO_3$ inhibited undesired pyrochlore phase growth[55]. Ca and Sr-incorporated $PrMnO_3$ were examined at 1000°C, with Ca-doped $PrMnO_3$ exhibiting higher conductivity (266 S cm^{-1}) than Sr-added $PrMnO_3$. However, the TEC of 30 mol% Ca-incorporated $PrMnO_3$ ($11.9\times10^{-6}K^{-1}$) was

identical to Sr-substituted $PrMnO_3$[56]. Sr-incorporated $Pr_{0.8}Sr_{0.2}FeO_3$ displayed conductivity of 300 S cm^{-1} at 550°C, dropping to 78 S cm^{-1} at 800°C, with x=0.3-0.5 samples having electrical conductivity >100 S cm^{-1} and TEC matching YSZ ($12.1\times10^{-6}K^{-1}$)[57]. Pr^{3+} similar electro negativity to La^{3+}contributes to comparable TEC values[58]. Nd-based compounds have been extensively researched with various substituent at A and B-sites. Cobalt-absent$Nd_xSr_{1-x}Fe_{0.8}Cu_{0.2}O_{3-\delta}$ (x=0.3-0.7) were studied for structural, thermal, and electrochemical characteristics, with maximum conductivity (124 S cm^{-1}) observed for x=0.5 at 700°C, alongside a TEC of $14.7\times10^{-6}K^{-1}$, [59]. Kong and colleagues[60] explored crystal structure, TEC, electronic conductivity, and electrochemical characteristics of $NdBaCu_2O_{5+\delta}$ and $NdBa_{0.5}Sr_{0.5}Cu_2O_{5+\delta}$,with TEC values ($13\times10^{-6}K^{-1}$ and $14.5\times10^{-6}K^{-1}$) compatible with $Sm_{0.2}Ce_{0.8}O_{2-\delta}$electrolyte, and conductivity reaching 570 S cm^{-1} at 200°C. Gd-based $GdBaFeNiO_{5+\delta}$ exhibited average TEC of $14.7\times10^{-6}K^{-1}$ and conductivity similar to 9.5 Scm^{-1} at 400°C, less than cathode materials based on cobalt[61]. Ba, Nd, and Gd-based cathode materials display TEC comparable to YSZ and other electrolytes but lower conductivity compared to cobalt-based counterparts. This limits their applicability as SOFC cathodes, especially in IT-SOFCs. While these materials offer promising attributes such as lower cost and enhanced stability, their lower conductivity poses a challenge for widespread adoption in SOFC technology. Additional research and improvements steps are essential to address these limitations and open the full capability of cobalt-absent perovskitecathode materials for SOFC applications.

9 Alkaline-earth-based Materials

Cobalt-absent Ti-incorporated $SrFe_{1-x}Ti_xO_{3-\delta}$ compounds, synthesized via the solid-state route technique, demonstrate compatibility with $La_{0.9}Sr_{0.1}Ga_{0.8}Mg_{0.2}O_{3-\delta}$ and $Ce_{0.8}Sm_{0.2}O_{1.9}$ electrolytes [62]. Conductivity values vary with Ti content (x = 0.00-0.15), with the specimen having x=0.05 exhibiting the maximum conductivity of 72 S cm^{-1} at 650°C. Conductivity behavior indicates a semiconductor to metallic phase change. Average TEC diminished from $26.5\times10^{-6}K^{-1}$ to $22.9\times10^{-6}K^{-1}$ with increasing Ti quantity, attributed to stronger Ti-O bonds compared to Fe-O bonds. These TEC values are similar to systems like $Sr_{0.97}Te_{1-x}Fe_xO_{3-\delta}$, $La_{1-x}Sr_xFe_{1-y}Ti_yO_{3-\delta}$, and $La_{0.6}Sr_{0.4}Ti_xFe_{1-x}O_{3-\delta}$[63]. Li *et.al.*[64] investigated $SrFe_{0.7}Cu_{0.3}O_{3-\delta}$ oxide's electrochemical performance, yielding conductivity values between 25-54S cm−1 at 500-800°C. The TEC curve, obtained from 50-800°C in air, yielded a mean value of $13.8\times10^{-6}K^{-1}$, harmonious with $Ce_{0.9}Gd_{0.1}O_{1.95}$ electrolyte. Cu doping, instead of Ti, significantly reduced the system's TEC without much impact on conductivity. Ding *et.al.*[65] explored $Sr_{0.7}Y_{0.3}CuO_{2+\delta}$, exhibiting a TEC of $11.1\times10^{-6}K^{-}1$ from 25-800°C, comparable to SDC electrolyte ($12.1\times10^{-6}K^{-1}$). TEC values notably less than another lanthanum-founded compounds like $Ln_{0.6}Sr_{0.4}CoO_{3-\delta}$ and $LnBaCo_2O_{5+\delta}$[66]. Khartonet.*al*. evaluated $SrTi_{1-x}Fe_xO_{3-\delta}$'s thermal and transport properties, noting TEC values of $11.7-13.8\times10^{-6}K^{-1}$ in the temperature span of 300-700°C. Increasing Fe quantity at the B-site increased ionic and electronic conductivity due to reduced volume of cubic primitive cell and ion transference number <0.1. $Sr_{1-x}Ce_xMnO_3$ ($0 \le x \le 0.5$) structural, thermal, and electrical characteristics were examined by Ding and coworkers[65], revealing a tetragonal stable structure with high conductivity (290 S cm^{-1} at 1000°C) and a first-order deviation toward cubic structure from tetragonal structure in $Sr_{1-x}Ce_xMnO_{3-\alpha}$ (x=0.1, 0.3), reaching a heightened conductivity of 450 S cm^{-1} at 150°C[67]. Another extensively studied Sr-based material is $SrZrO_3$, investigated by Misra *et al*. for its electrical conductivity and oxygen monitoring capability in $SrZr_{1-x}Fe_xO_{3-\delta}$ ceramics. Semiconducting behavior was observed, with conductivity between 10−9.5 to 10−8.0 S cm^{-1} at 200-527°C, and configuration with x=0.1 and x=0.2 exhibiting the highest deviation in conductivity similar to 400%. Fe substitution for Zr led to reduced grain size, indicating potential improvements in crystallization temperature or inhibition of grain growth. $SrZrO_3$ exhibited lower conductivity values compared to $SrTiO_3$. $SrFe_{1-x}NbxO_3$ also reported reduce conductivity and elevated TEC values, indicating limited potential compared to $SrZr_{1-x}Ni_xO_3$[68]. Overall, Sr-founded materials demonstrate favorable conductivity comparable to standard electrolytes like YSZ, while their TEC values are also competitive. These materials hold promise for various applications, including SOFCs, due to their favorable electrical and thermal properties. Zhang and colleagues [69]utilize a sol-gel method to fabricate $SrFeO_{3-\sigma-\delta}F_\sigma$ (SFFσ, σ = 0, 0.05, and 0.10) and $SrFe_{0.9}Ti_{0.1}O_{3-\sigma-\delta}F_\sigma$ (SFTFσ, σ = 0, 0.05, and 0.10) perovskite oxy-fluorides, using EDTA-CA (ethylene-diaminetetra-acetic acid-citric acid) as a combined agent to enhance electrochemical performance. These

materials exhibited improved O_2 reduction reaction activity and stability due to appropriate anion doping, facilitating enhanced bulk diffusion at intermediate temperatures. ASR values of 0.875, 0.393, and 0.491 Ω cm^2 were attained at 600°C in air for $SrFeO_{3-\delta}$, $SrFeO_{2.95-\delta}F_{0.05}$, and $SrFeO_{2.90-\delta}F_{0.10}$, respectively. Li and colleagues developed Ta and Nb co-substituted $SrCo_{0.8}Nb_{0.1}Ta_{0.1}O_{3-\delta}$ (SCNT) perovskite compound via solid-state technique for cathodic applications. The substitution of Nb and Ta facilitated a collaborative atmosphere, prompting surface electron transfer, enhancing ionic mobility, and generating O_2 vacancies, particularly at temperatures ≤ 500°C. In an anode-sustained GDC-founded symmetrical fuel cell, the material exhibited ASR of approximately 0.16 and 0.68 Ω cm^2 with elevated power densities of 1.2 and 0.7 W/cm^2 at 500 and 450°C, alternately. Hussain and colleagues[70] fabricate $La_xSr_{1-x}Fe_{1-y}Cu_yO_{3-\delta}$ (x =0.54, 0.5, y = 0.2, 0.4) perovskite structures via a sol-gel technique, among which $La_{0.54}Sr_{0.46}Fe_{0.80}Cu_{0.20}O_{3-\delta}$ exhibited outstanding performance and conductivity. This composition attained an elevated power density of 452 mW/cm^2 and an elevated conductivity of 9.029 S/cm at 600°C.

10 Conclusion

This review article summarizes current research on cathode materials for SOFCs, highlighting perovskite materials as promising candidates due to their excellent conductivity. Specifically, $La_{1-x}Ca_xFeCoO_3$ and $La_{1-x}Sr_xYCoO_3$ are identified as having the potential for desired conductivity and operational temperatures, with the possibility of further enhancement through compositional adjustments. The study also evaluates recent advancements in nanomaterials. Emphasis is placed on developing cathode materials with high electrical conductivity to lower SOFC operating temperatures, thereby enhancing usability and reducing operational expenses. This synthesis underscores the importance of ongoing research in optimizing cathode materials for SOFCs to advance the technology's efficiency and cost-effectiveness on a global scale.

References

1 Bamburov A, Naumovich Y, Khalyavin D D & Yaremchenko A A, *Chem Mater,* 35 (2023)8145.
2 Devi S, Ahmed N, Manokamna, Singh A & Paul S, *Mater Today Proc,* 60 (2022) 1989.
3 Paul S, Ahmed N, Mano kamna, Sen A, Rialach S, Sharma N & Devi S, *Ind J Phys*, 98 (2024) 4711.
4 Ahmed N, Devi S, Dar M A, Ibrahim S K M, Sharma A, *et.al*, *Ind J Phys,* 98 (2024) 877.
5 Sen A, Paul S, Rialach S, Shaheen K, Prerna S, Manokamna, Sharma P & Bhargava G, Phys Solid State, 67 (2025) 338.
6 Bessler W G, Vogler M, Störmer H, Gerthsen D, Utz A, Weber A, *et.al.*, *Phys Chem,* 12(2010) 13888.
7 Paul S, Ahmed N, Sen A, Rialach S, Devi S & Manokamna, *Indian J Phys*, 99 (2025) 2475.
8 Lohmann F P, Schulze P S C, Wagner M, Naumov O, Lotnyk A & Abel B, *Mater Chem A,*5 (2017) 15021.
9 Sen A & PaulS, *MRS Advances*, (2025) doi: 10.1557/s43580-024-01102-w.
10 Jiang S P, *J Mater Sci,* 43 (2008) 6799.
11 Mahato N, Banerjee A, Gupta A, Omar S & Balani K, *Prog Mat Sc,* 72 (2015) 141.
12 Sen A, Paul S, Diksha, Malavika, Kumar R, Mujawar A M, Sharma V & Bhargava G, *Ceramics Int*, (2025), https://doi.org/10.1016/j.ceramint.2025.06.389
13 Rialach S, Gautam S, Goyal N & Paul S, *Synthetic Metals*, 312 (2025) 117871.
14 O'Hayre R, Barnett D M & Prinz F B, *J Electro chem. Soc,* 152A (2005) 439.
15 Sun C, Hui R & Roller J, *J Solid State Electrochem,* 14 (2010) 1125.
16 Devi S, Ahmed N, Sharma N, Manokamna, Sen A, Rialach S & PaulS, *Rasayan J Chem,* 17 (2024) 1110.
17 Zaccaria V, Tucker D, Traverso A, *J Power Sources,* 311 (2016) 175.
18 Zarabi Golkhatmi S, Asghar M I & Lund P D, *Renew Sustain Energy Rev*, 161 (2022) 112339.
19 Rialach S, Gautam S, Goyal N& Paul S, *Electrochimica Acta*,524(2025) 145976.
20 Yang B, Wang J , Zhang M, Shu H, Yu T, Zhang X, Yao W & Sun L, *Energy Convers Manag,* 213 (2020) 112856.
21 Istomin S Y & Antipov E V, *Russ Chem Rev,* 82 (2013) 686.
22 Bie K, Fu P, Liu Y & Muhammad A, *J Power Sources,* 460 (2020) 228101.
23 Haverkort M W, Hu Z, Cezar J C, Burnus T, Hartmann H, Reuther M, *et. al., Phys Rev Lett,* 97 (2006) 176405.
24 Gautam S, Rialach S, Paul S & Goyal N, *RSC Adv*, 14 (2024) 14311.
25 Han N, Shen Z, Zhao X, Chen R & Thakur V K, *Sci Total Environ*, 806 (2022) 151213.
26 Ke M, Wang W, Yang X, Li B & Li H, *Ceram Int*, 48 (2022) 8709.
27 Kim J-H & Manthiram A, *J Electrochem Soc,* 155(2008) B385.
28 Zhou Q, Wei W C J, Guo Y & Jia D, *Electro chem Comm,* 19 (2012) 36.
29 Shen F & Lu K, *Electrochim Acta,* 211(2016) 445.
30 Wu Y-C, Huang P-Y & Xu G, *Ceramics Int,* 43 (2017) 2460.
31 Li X, Jiang X, Pang S, Wang Q, Su Z & Zhang Q, *Int J Hydrogen Energy,* 36 **(**2011**)** 13850.
32 Gędziorowski B, Świerczek K & Molenda J, *Solid State Ion,* 225 (2012) 437.
33 Dasgupta N, Krishnamoorthy R & Jacob K T, *Mater Sci Eng, B* 90(2002) 278.
34 Kim J H & Irvine J T S, *Int J Hydrogen Energy,* 37 (2012) 5920.
35 Kim J, Choi S, Park S, Kim C, Shin J & Kim G, *Electrochimica Acta*, 112 (2013) 712.
36 Yi K, Sun L, Li Q, Xia T, Huo L, Zhao H, *et. al., Int J Hydrogen Energy,* 41 (2016) 10228.

37 Donazzi A, Pelosato R, Cordaro G, Stucchi D, Cristiani C, Dotelli G, *et. al., Electrochim Acta,* 182 (2015) 573.
38 Devi S, Manokamna, Kumar R & Paul S, *Mater Today Proc,* (2023). https://doi.org/10.1016/j.matpr.2022.12.132
39 Mizusaki J, Tabuchi J, Matsuura T, Yamauchi S & Fueki K, *J Electrochem Soc,* 136 (1989) 2082.
40 Tai L, *Solid State Ionics,* 76 (1995) 259.
41 Paul S, *Mater Today Proc,* (2023). https://doi.org/10.1016/j.matpr.2023.02.418
42 Teraoka Y, Nobunaga T, Okamoto K, Miura N & Yamazoe N, *Solid State Ionics,* 48 (1991) 207.
43 Manokamna, Paul S, Singh A, Singh K L, Bhargava G & Singh A P, *Rasayan J Chem,* 14 (2021) 1019.
44 Paul S, Manokamna, Kumar A, Kaur S, Singh A & Kumar A, *Mater Today Proc,* 56 (2022) 1684.
45 Jo S H, Muralidharan P & Kim D K, *Electrochem Commun,*11(2009) 2085.
46 Li N, Lü Z, Wei B, Huang X, Chen K, Zhang Y, *et. al., J Alloys Compd,* 454 (2008) 274.
47 Zhou Q, Zhang Y, Shen Y & He T, *J Electrochem Soc,* 157 (2010) B628.
48 Kuroda C, Zheng K & Świerczek K,*Int J Hydrogen Energy,* 38 (2013) 1027.
49 Phillipps M, *Solid State Ion,* 123 (1999) 131.
50 Yokokawa H, *Solid State Ion,* 40 **(**1990) 398.
51 Sahini M G, Mwankemwa B S & Kanas N, *Ceramics Int*, 48 (2022) 2948.
52 Hussain A, Song R-H, Kim T, Mehdi A M, Shin J, Kwon B-S, Ali M M, Joh D W, Khan M Z, Hong J-E, Lee S & Lim T-H, *ECS Trans,* 111 (2023) 1535.
53 Ishiham T, Kudo T, Matsuda H & Takita Y, *J Am Ceram Soc,* 77(1994) 1682.
54 Sakaki Y, Takeda Y, Kato A, Imanishi N, Yamamoto O, Hattori M & Esaki Y, *J Jpn Soc Powder Metallurgy,* 46 (1999) 293.
55 Rim H-R, Jeung S-K, Jung E & Lee J-S, *Mater Chem Phys,* 52 (1998) 54.
56 Piao J, Sun K, Zhang N, Chen X, Xu S & Zhou D, *J Power Sources,* 172 (2007) 633
57 Simner S P, Bonnett J F, Canfield N L, Meinhardt K D, Sprenkle V L & Stevenson J W, *Electrochem Solid State Lett,* 5 A (2002) 173.
58 Yin J-W, Yin Y-M, Lu J, Zhang C, Minh N Q & Ma Z-F, *J Phys Chem, C* 118 (25) (2014) 13357.
59 Kong X, Liu G, Yi Z & Ding X, *Int J Hydrogen Energy,* 40 (2015) 16477.
60 Li L, Jin F, Shen Y &He T, *Electrochim Acta*, 182 (2015) 682.
61 Yu X, Long W, Jin F &He T, *Electrochim Acta,* 123 (2014) 426.
62 Tsipis E V, Patrakeev M V, Kharton V V, Yaremchenko A A, Mather G C, Shaula A L, *et. al.*, *Solid State Sc,* 7 (2005) 355.
63 Li Q, Xia T, Sun L, Zhao H & Huo L, *Electrochim Acta,* 150 (2014) 151.
64 Ding X, Gao X, Shen J, Wang J, Zhu W, Wang X, *et. al.*, *Int J Hydrogen Energy,* 39 (2014) 1030.
65 Lee K T & Manthiram A, *J Electrochem Soc,* 153A (2006) 794.
66 Hashimoto S & Iwahara H, *J Electroceram,* 4 (2000) 225.
67 Kaur P & Singh K, *ECS Trans,* 91 (2019) 1543.
68 Zhang Z, Zhu Y, Zhong Y, Zhou W & Shao Z, *Adv Energy Mater,* 7 (2017) 1700242.
69 Hussain M, Muneer M, Abbas G, Shakir I, Iqbal A, Javed M A, *et. al., Ceramics Int,* 46 (2020) 18208.